

## Supporting Information

### **Construction of MAPbBr<sub>3</sub>/BiFeO<sub>3</sub> Z-scheme heterojunction and the enhanced piezo-photocatalytic performance**

Dan-Yang Zhou, Yi-Ou Zhou, Su-Yan Fang, Guang-Yu Pan, Xiong He, Mei-Ling Xu, Fu-Tian Liu\* and  
Kui Li\*

School of Materials Science and Engineering, University of Jinan, Jinan, 250022, PR China.

Email: mse\_liuft@ujn.edu.cn, mse\_lik@ujn.edu.cn

# 1. Experimental Section

## 1.1 Materials

Methylammonium bromide (MABr, 99.5%, CAS 6876-37-5), Lead bromide ( $\text{PbBr}_2$ , 99.0%, CAS 10031-22-8), Iron chloride hexahydrate ( $\text{FeCl}_3 \cdot 6\text{H}_2\text{O}$ , 98%, CAS 10025-77-1), Bismuth nitrate pentahydrate ( $\text{Bi}(\text{NO}_3)_3 \cdot 5\text{H}_2\text{O}$ , 99%, CAS 10035-06-0), Sodium Hydroxide (NaOH, 97%, CAS 1310-73-2) Hydrobromic acid (HBr, 40%, CAS 10035-10-6) were purchased from Shanghai Macklin Biochemical Co., Ltd. Ammonia solution ( $\text{NH}_3 \cdot \text{H}_2\text{O}$ , 25-28%, CAS 1336-21-6), Ethanol (99.7%, CAS 64-17-5), Isopropyl alcohol (99.5%, CAS 67-63-0) were purchased from Tianjin Fuyu Fine Chemical Co., Ltd. All chemicals were used without further purification. All of the reagents and solvents were commercially available and could be used without further purification.

## 1.2 Synthesis of $\text{MAPbBr}_3$

$\text{MAPbBr}_3$  nanocrystals were prepared by high-energy ball milling. MABr and  $\text{PbBr}_2$  were weighed in a molar ratio of 1 : 1, and then placed in 3 mL of IPA to disperse uniformly by ultrasonic. As a grinding agent, IPA can achieve sufficient grinding. It was then transferred to a 25 mL agate grinding jar containing 5 agate grinding balls, and ground for 120 min at 600 rpm in a glove box under  $\text{N}_2$  atmosphere. After ball milling, the orange-yellow perovskite paste was centrifuged and washed with IPA for more than three times to remove unreacted substances, followed by vacuum drying at 60 °C to obtain orange-yellow  $\text{MAPbBr}_3$  powder.

## 1.3 Synthesis of $\text{BiFeO}_3$ nanosheets

$\text{BiFeO}_3$  nanosheets were synthesized via solvothermal and subsequent annealing following the previously reported document with some slight modifications. In short, 3 mmol  $\text{Bi}(\text{NO}_3)_3 \cdot 5\text{H}_2\text{O}$  was completely dissolved in 100 mL ethylene glycol solution under vigorous stirring. Then, the mixture of 2.5 mmol  $\text{FeCl}_3 \cdot 6\text{H}_2\text{O}$  and 100 mL

deionized water was added to the above solution. The pH value of the mixed solution was adjusted to be 10~11 by dropping  $\text{NH}_3 \cdot \text{H}_2\text{O}$  under vigorous stirring for 1h. The sediment was collected by centrifugation, then added to 20 mL of NaOH solution (5 mol/L) and transferred to a 50 mL Teflon-lined autoclave and heated for 48 h under 180 °C. Afterwards, the red powder was collected by centrifugation and washed several times with ethanol and deionized water, and then dried in a vacuum oven at 60 °C overnight. Finally, the products were annealed under an air atmosphere at 500 °C (2 °C  $\text{min}^{-1}$ ) for 2 h to gain  $\text{BiFeO}_3$ .

#### *1.4 Synthesis of $\text{MAPbBr}_3/\text{BiFeO}_3$*

MABr and  $\text{PbBr}_2$  were weighed in a molar ratio of 1 : 1, which reagent is weighed in 4 parts and, and then placed in 3 mL of IPA to disperse uniformly by ultrasonic. Then, 0.5, 1, 1.5 and 2 mg of prepared  $\text{BiFeO}_3$  nanosheets were weighed and put into the above four solutions respectively. In the same method as  $\text{MAPbBr}_3$  preparation, the samples were ball milling for 120 min at a rotating speed of 600 rpm. After ball milling, the orange-yellow perovskite paste was centrifuged and washed with IPA for more than three times to remove unreacted substances, followed by vacuum drying at 60 °C to obtain  $\text{MAPbBr}_3/\text{BiFeO}_3$  powder.

#### *1.5 Materials Characterization*

The phase composition of samples was obtained by X-ray diffraction (XRD, D8 Advance) equipped with Cu  $K\alpha$  radiation ( $\lambda = 1.54060 \text{ \AA}$ ). Fourier transform infrared spectroscopy (FT-IR) was collected on a Thermo Scientific Nicolet iS10 spectrometer. The morphologies and compositions of samples were observed on field emission scanning electron microscope (SEM, Gemini300, Carl Zeiss) and transmission electron microscopy (TEM, JEM-2100Plus, JEOL). The X-ray photoelectron spectroscopy (XPS) spectra were analyzed by a Thermo Fisher Scientific corporation Escalab 250Xi instrument. UV-vis DRS spectra was measured with Shimadzu UV-3600. Steady photoluminescence (PL) emission spectra were tested by a luminescence spectrophotometer (QM-400, PTI) with 450 nm excitation wavelength. Transient time

resolved PL decay measurements were obtained using an FLS1000 under the excitation of 405 nm.

### *1.6 Photocatalytic Experiments*

The CO<sub>2</sub> reduction performance was evaluated under the irradiation of ultrasonic (40 kHz, 100 W), visible light ( $\lambda \geq 420$  nm) and the combined ultrasonic and visible light. To be specific, 20 mg powder sample was weighed and placed in a quartz reactor filled with CO<sub>2</sub>, the test liquid was a 10 mL mixture of toluene and isopropyl alcohol (v : v = 9 : 1). Test the gas products every hour under the visible light of 300 W Xe lamp. H<sub>2</sub> and CO CH<sub>4</sub> content were analyzed by gas chromatography (GC-7900, CEAULight, China) with a TCD and FID detector. In experiments investigating the effect of pH on performance, the pH is adjusted to 4 or 12.9 by using HBr or NaOH.

### *1.7 Electrochemical measurements*

Photoelectrochemical characterizations were proceeded in Tetrabutylammonium hexafluorophosphate (TBAPF<sub>6</sub>) (0.1 M) solution with a standard three-electrode system on the electrochemical station (SP-150, Bio-Logic). The carbon cloth coated with catalyst, carbon rod and saturated Ag/AgCl were served as working electrode, counter electrode and reference electrode, respectively. Typically, a slurry of 4 mg of sample and 1 mL of ethanol were used to make the working electrode. The electrochemical impedance spectroscopy (EIS) was recorded from 0.01 Hz to 100 kHz with a sinusoidal ac perturbation of 10 mV. The impedance potential model was employed to collect the Mott-Schottky plots with the frequency of 500, 1000 and 2000 Hz. I-t curves were recorded using 300 W Xe lamp with a 420 nm cutoff filter.

## 2. Supporting Figures

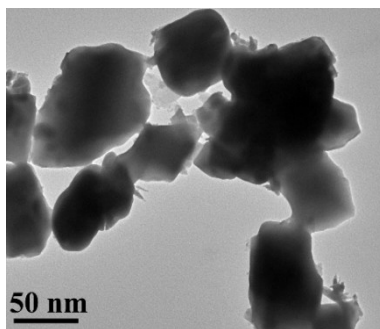


Fig. S1 TEM image of MAPbBr<sub>3</sub>

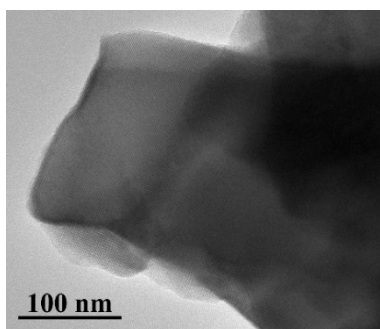


Fig. S2 TEM image of BiFeO<sub>3</sub> nanosheet

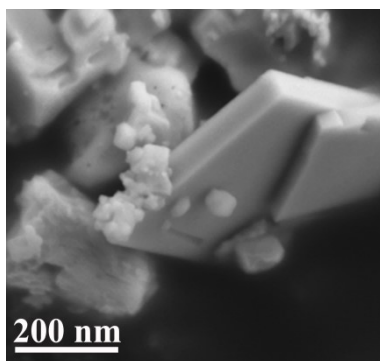


Fig. S3 SEM image of MAPbBr<sub>3</sub>/BiFeO<sub>3</sub>

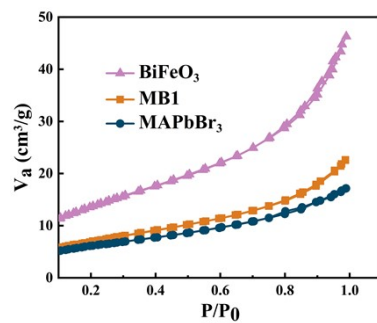


Fig. S4 N<sub>2</sub> adsorption - desorption isotherms of BiFeO<sub>3</sub>, MAPbBr<sub>3</sub>/BiFeO<sub>3</sub> 1 and MAPbBr<sub>3</sub>.

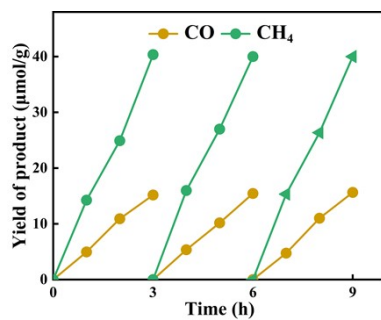


Fig. S5 Recycling test of MB1 within 9h.

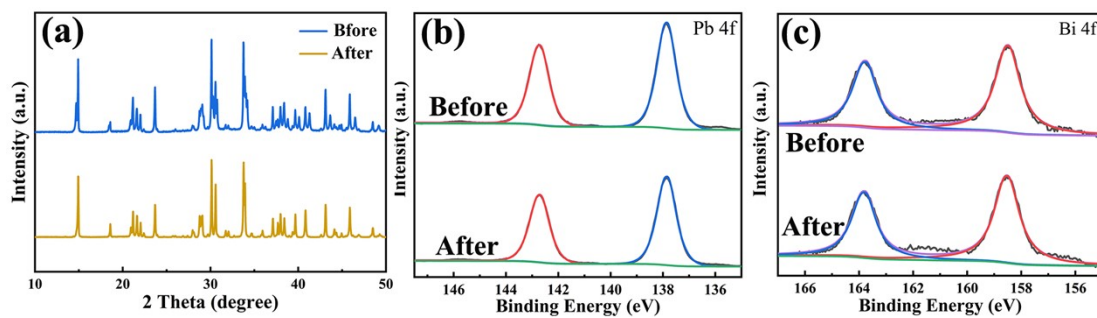
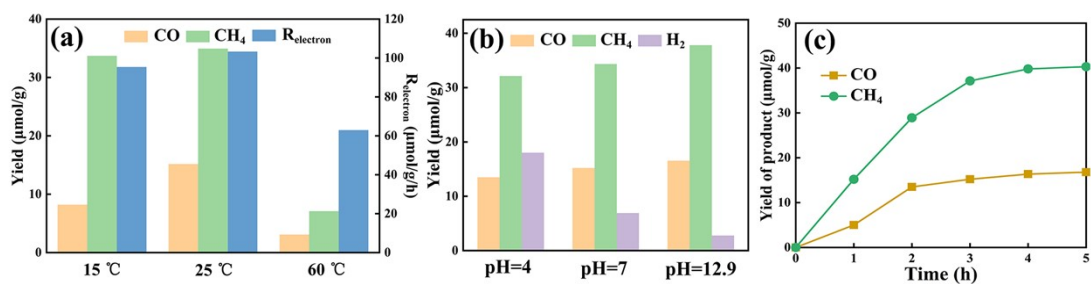


Fig. S6 Cycle stability of photocatalytic CO<sub>2</sub> reduction of MB1: the (a) XRD spectra; the XPS survey of (b) Pb 4f and (c) Bi 4f.



**Fig. S7** Product yield of piezo-photocatalytic products of MB1 at different (a) pH and (b) temperature within 3h; (c) The yield of piezo-photocatalytic products of MB1 at pH=12.9.

### 3. Supporting Tables

Table S1 Specific surface area data of samples

Sample	S <sub>BET</sub> (m <sup>2</sup> g <sup>-1</sup> )	S <sub>Langmuir</sub> (m <sup>2</sup> g <sup>-1</sup> )
MAPbBr <sub>3</sub>	13.47	54.8
MB1	21.36	84.19
BiFeO <sub>3</sub>	41.2	197.54

Table S2. The detailed transient fluorescence properties of MAPbBr<sub>3</sub>, BiFeO<sub>3</sub> and MB1 samples.

Samples	A <sub>1</sub> (%)	τ <sub>1</sub> (ns)	A <sub>2</sub> (%)	τ <sub>2</sub> (ns)	A <sub>3</sub> (%)	τ <sub>3</sub> (ns)	Average lifetime τ (ns)
MAPbBr <sub>3</sub>	44.3	1.79	31.8	1.79	23.9	2.05	1.86
MB1	47.9	1.52	51.9	1.52	0.17	7.25	0.81
BiFeO <sub>3</sub>	60.9	1.52	39.0	3.59	0.02	14.5	1.23

Table S3 Resistance value (Rs and Rc) of MAPbBr<sub>3</sub>, MB1 and BiFeO<sub>3</sub> samples.

Sample	R <sub>s</sub> (Ω)	R <sub>c</sub> (Ω)
MAPbBr <sub>3</sub>	117	2994
MB1	54.1	1576
BiFeO <sub>3</sub>	138.6	3247



Table S4 Calculated apparent quantum field (AQY) of MB1 sample at different wavelengths

Wavelength (nm)	R <sub>electron</sub> (μmol/h)	Light Intensity (mW)	AQY (%)
420	42.4	92.5	3.6
475	40.39	129.9	3.4
550	7.46	148.4	0.63
650	0.52	116.6	0.043

The AQY was calculated following equation:

$$\text{AQY} = \frac{\alpha \times \text{amount of gas molecules evolved}}{\text{Total photons incident}} \times 100\%$$

$$= \frac{\alpha \times (N \times N_A \times h \times c)}{I \times S \times t \times \lambda} \times 100\%$$

$\alpha=2$  or  $8$  for the CO and CH<sub>4</sub> evolution, respectively. Where  $N_A$  is the Avogadro constant ( $6.02 \times 10^{23}$ ),  $h$  is the Planck constant ( $6.62 \times 10^{-34}$  J·s),  $c$  is the speed of light ( $3 \times 10^8$  m·s<sup>-1</sup>),  $I$  is the light intensity ( $\text{W cm}^{-2}$ ),  $S$  is the irradiation area ( $\text{cm}^{-2}$ ,  $7.065 \text{ cm}^{-2}$ ),  $t$  is the photocatalytic reaction time (s),  $\lambda$  is the wavenumber of the monochromatic light (m).

Table S5 Comparison of photocatalytic CO<sub>2</sub> reduction rate over halide perovskite-based photocatalysts.

Photocatalytic	Reaction medium	Products	Test Time (h)	R <sub>electron</sub> (μmol/g/h)	References
MAPbBr <sub>3</sub> /BiFeO <sub>3</sub>	toluene/isopropanol	CO, CH <sub>4</sub>	9	113.2	<b>This work</b>
Re(CO) <sub>3</sub> Br(dcbpy) on CsPbBr <sub>3</sub>	toluene/isopropanol	CO	15	71.4	<i>Sol. RRL</i> 2019, <b>4</b> , 1900365.
CsPbBr <sub>3</sub> NCs/Bi <sub>2</sub> WO <sub>6</sub>	acetonitrile/water	CO, CH <sub>4</sub>	10	114.4	<i>ACS Appl. Mater. Interfaces</i> 2020, <b>12</b> , 31477-31485.
CsPbBr <sub>3</sub> /USGO/α-Fe <sub>2</sub> O <sub>3</sub>	acetonitrile/water	CO	4	146	<i>Small</i> 2020, <b>16</b> , 2002140.
CsPbBr <sub>3</sub> QDs on Mxene	ethyl acetate/water	CO, CH <sub>4</sub>	12	110.64	<i>J. Phys. Chem. Lett.</i> 2019, <b>10</b> , 6590-6597.
MAPbI <sub>3</sub> QDs @PCN-221(Fex)	ethyl acetate/water	CO, CH <sub>4</sub>	80	112.32	<i>Angew. Chem. Int. Ed.</i> 2019, <b>58</b> , 9491-9495.